University of Thi-Qar Journal of Science (UTJsci)
E-ISSN: 2709-0256, P-ISSN: 1991-8690, Vol. 10, No. 2, Dec. 2023

Cross gain modulation in quantum dot semiconductor optical amplifiers under the influence of the Probe

1st Ahmed H. Flayyih
Applied Geology Department
College of Science/ University of Thi-Qar
Nasiriya/ Iraq
ahmed.hmood_ph@sci.utq.edu.iq

2nd Seyedeh Hamideh Kazemi
Department of Physics/ University of Zanjan
Zanjan/ Iran
s.h.kazemi@znu.ac.ir

3rd Amin H. Al-Khursan
Nasiriya Nanotechnology Research Laboratory (NNRL)/ College of Science/ University of Thi-Qar,
Nasiriya/ Iraq
ameen_2all@yahoo.com

Received: 2023-11-16, Revised: 2023-12-07, Accepted: 2023-12-12, Published: 2023-12-26

***Abstract*—The Pulse effect on the cross-gain modulation (XGM) in the quantum dot (QD) semiconductor optical amplifiers (SOAs) is investigated using the combining of the SOA power with the QD rate equations system. The QDs structure includes three regions: ground state (GS), excited state (ES) and wetting layer (WL). Thus, a set of rate equations for pump and probe signals is introduced for both steady-state and small-signal power values, which are solved numerically. The pulse shape was included in the analysis, for pump and probe signals. The theoretical results showed a good agreement with the experimental results. It was found that decreasing pulse width of pump/probe ratio is efficient to increase XGM efficiency and bandwidth.**

Keywords: quantum dot, semiconductor optical amplifier, cross gain modulation XGM.

I. INTRODUCTION

Recently, w wavelength conversion techniques attract a great interest due to their all-optical potential applications [1]. One of the most semiconductor optical amplifiers (SOAs) processes, which is considered as the key device for all-optical convertors, is the cross-gain modulation (XGM) [2-4]. In XGM, the SOA gain of a weaker probe is modulated by a strong pump signal, and then transferring information with the pump signal to the probe. Thus, the data are converted from pump to probe wavelength [5] and the conversion takes place without modifying the data content of the signal [6-8]. An important advantage in XGM is that the input power of the optical signal has a large dynamic range. It is relying on the modulation of the carrier density and is thus limited by the relatively slow carrier generation and recombination rates [9]. For bulk and quantum well (QW) SOAs, when the bit period is close to gain recovery time of the SOA, a crosstalk penalty results between the multiplexed input signals change in their active regions [10,11]. Another XGM discontinuity is the degradation of the extinction ratio of the upconverted signal [5]. In bulk and QW SOAs, the dominant gain recovery mechanism is the total carrier density depletion which is slow. This limitation can be overcome by the use of quantum dot (QD) SOAs which are predicted to have an ultrafast gain recovery time due to the dominance of spectral hole burning (SHB) mechanism [12-13].

It is demonstrated that the use of QD SOAs improves XGM characteristics. The pattern-free effect is demonstrated by the high gain or low dot density [13]. The gain recovery is enhanced by the carrier relaxation from excited state (ES) to the ground state (GS) in the QD [14]. Additionally, QDs have both homogenous and inhomogeneous broadenings of gain so that broadband XGM is possible [15]. XGM has been discussed extensively during the last decades. XGM in p-doped QD SOAs was reported [12]. Error-free 320 Gb/s operation is presented [16]. XGM in columnar QD SOAs was also reported experimentally [17]. Different approaches and wide structures were discussed [4, 12, 18].

Studies on theory of XGM in QD SOAs follows the method reported in [19, 20]. In their works, the small-signal analysis was s done for QD SOA and a rate equation for small-signal power in both pump and probe were calculated. The steady-state part for power was defined by a rate equation of power (Eq.4) , but this is not the adequate case since there is a correlation between small-signal and steady-state parts of power, as we can see in Eq. (11) below. So, an adequate definition for the steady-state power rate equation was undertaken here. Additionally, pulse shape was introduced through our analysis of power which is important to be covered in SOA processes analysis. These point represents the difference between our work and others. Thus, in our analysis, here, a set of four rate equations system for steady-state and small-signal powers for both

https://doi.org/10.32792/utq/utjsci/v10i2.1132

pump and probe were obtained. Then, they were solved numerically to get the efficiency. When these equations were connected with the QD SOA rate equations, a form covers the most important factors into QD SOA work was introduced. The results from our model were compared with the experimental result in [19] and a good a agreement was shown. This work was organized as follow: in section 2, XGM analysis is presented. In section 3, the conversion efficiency is defined while the small-signal theory for XGM is states. The simulated QD structure in this study was described in section 5. Section 6 presents the results and the discussion. Finally, The conclusions from this work are drown in section 7.

II. Theoretical analysis of XGM in QD SOAs

Theory of XGM in QD SOAs based on QD rate equations has been developed in different works [12, 13, 18, 21]. The carrier dynamics were described by the rate equations for electrons in GS, ES, and WL which is serving as a carrier reservoir [14]. This is because of the larger effective mass of holes and lower quantization energies of QD levels in the valence band, and that led to a faster relaxation of holes. Therefore, electrons' behavior limits dynamics of the carrier. It was assumed that carriers were injected directly from the contacts into WL and thus, the barrier dynamics are ignored [18]. The rate equations in the QD SOA can be written as [6]

$$\frac{dN_w}{dt} = \frac{J}{e\,L_w} - \frac{N_w(1-h)}{\tau_{w2}} + \frac{N_w\,h}{\tau_{2w}} - \frac{N_w}{\tau_{wr}} \quad (1)$$

$$\frac{dh}{dt} = \frac{N_w L_w (1-h)}{NQ\,\tau_{w2}} + \frac{f(1-h)}{\tau_{12}} - \frac{N_w L_w\,h}{NQ\,\tau_{2w}} - \frac{h(1-f)}{\tau_{21}} \quad (2)$$

$$\frac{df}{dt} = \frac{h(1-f)}{\tau_{21}} - \frac{f(1-h)}{\tau_{12}} - \frac{f^2}{\tau_{1r}} - a_0\left(2f-1\right)P_{p,s} \quad (3)$$

where

$$a_0 = \frac{g_{p,s} L\,c}{\hbar\omega_{p,s}\upsilon_g A_{eff} NQ\sqrt{\varepsilon_r}}$$

N_w is the carrier density in WL. F and h are occupation probabilities in GS and ES respectively, e is the electron charge, τ_{w2} is the carrier relaxation time from WL to the ES, τ_{2w} is the carrier escape time from ES to WL, τ_{wr} τ_{1r} are the spontaneous radiative lifetimes in WL and QDs, respectively. NQ is the surface density of QDs, L_w is the effective thickness of the active layer, τ_{21} is the carrier relaxation time from ES to GS, and τ_{12} is the carrier escape time from GS to ES. The power along the amplifier length is obtained from the equation [6],

$$\frac{\partial P_{p,s}}{\partial z} = \left(\Gamma g(z,t) - \alpha_l\right)P_{p,s} \quad (4)$$

$P_{p,s}$ are pump and signal powers, respectively, α_l is the material loss, z is the distance in the longitudinal direction where (z=0) is the input facet and the output facet is at (z=L), L is the length of the SOA, $g(z,t)$ is the gain and is expressed as $g(z,t) = g_{\max}(2f-1)$, where $g_{\max}$ is the maximum gain. The solution of Eq. (4) is obtained by integration as follows [6],

$$P_{out} = P_{in}\exp\left(\int_0^L \left(\Gamma g(z,t) - \alpha_l\right)dz\right) \quad (5)$$

P_{in} is the input power. This relation is, then, applied for both pump and probe powers, $P_{p,s}$. Note that P_{in} can be taken as a Gaussian pulse [8],

$$P_{in}(\tau) = P_0 e^{-\frac{1}{2}\left(\frac{\tau}{\tau_0}\right)^2} \quad (6)$$

τ_0 is the full width at half maximum (FWHM).

III. Small-signal theory of wavelength converters

The total power P, is the sum of the pump and probe signals which can be written as [6]

$$P = P_{T_0} + \Delta p\,e^{-i\omega t} + \Delta p^* e^{i\omega t} \quad (7-a)$$

$$P_{T_0} = P_{P_0} + P_{s_0} \quad (7-b)$$

$$\Delta p = p_p + p_s \quad (7-c)$$

Where P_{T_0}, P_{P_0}, P_{s_0} are the steady-state values of the total power, pump and probe powers, respectively. Δp, p_p and p_s are the small-signal values of the total power, pump and probe, respectively. Occupation probabilities of GS and ES, and WL carrier density are expanded in their small-signal forms as follows

$$f = f_0 + \Delta f\,e^{-i\delta t} + \Delta f^* e^{i\delta t} \quad (8)$$

$$h = h_0 + \Delta h\,e^{-i\delta t} + \Delta h^* e^{i\delta t} \quad (9)$$

$$N_w = N_{w,0} + \Delta N_w e^{-i\omega t} + \Delta N_w^* e^{i\omega t} \quad (10)$$

Substitute Eqs. (7)-(8) into Eq. (4), then, using the small-signal analysis, one can obtains the following equations for the steady-state term,

$$\frac{\partial P_{P_0,S_0}}{\partial z} = (\Gamma g_{\max}(2f_0-1)P_{P_0,S_0} + 2\Gamma g_{\max}\Delta f^*\Delta p_{p,s} + 2\Gamma g_{\max}\Delta f\,\Delta p_{p,s}^* - \alpha_l P_{P_0,S_0}) \quad (11)$$

for the terms that resonant with $\left(e^{-i\delta t}\right)$ one obtains

$$\frac{\partial \Delta p_{p,s}}{\partial z} = \begin{pmatrix} \Gamma g_{\max}\left(2f_0 - 1\right)\Delta p_{p,s} \\ +2g_{\max}\Gamma\Delta f \;\; P_{P_0,S_0} - \alpha_l \Delta p_{p,s} \end{pmatrix} \tag{12}$$

Eqs. (11) and (12) are a set of four equations for pump and probe signals. The calculation of Δf was done by substituting of Eq. (8) into Eq. (3) and separate the terms resonant with $e^{-i\delta t}$, then, the occupation probability variation was obtained,

$$\Delta f = \frac{-a_0\left(\left(2f_0 - 1\right)\Delta p\right)}{\begin{pmatrix} (-i\,\delta + \dfrac{h}{\tau_{21}} + \dfrac{(1-h_0)}{\tau_{12}} - \dfrac{1}{\tau_{1r}} \\ +2a_0 P_T - \dfrac{\Delta h}{\Delta f}\left(\dfrac{(1-f_0)}{\tau_{21}} + \dfrac{f_0}{\tau_{12}}\right)) \end{pmatrix}} \tag{13}$$

To calculate Δf, we need to know the variation ratio between GS and ES occupation probability $\frac{\Delta f}{\Delta h}$. From the small-signal analysis of Eq. (2), $\frac{\Delta f}{\Delta h}$ can be obtained. It was given by,

$$\frac{\Delta f}{\Delta h} = \frac{\begin{pmatrix} -i\,\delta + \dfrac{N_{w0}L_w}{NQ}\left(\dfrac{1}{\tau_{w2}} + \dfrac{1}{\tau_{2w}}\right) + \dfrac{f_0}{\tau_{12}} + \dfrac{(1-f_0)}{\tau_{21}} \\ -\dfrac{L_w}{NQ}\left(\dfrac{(1-h_0)}{\tau_{w2}} - \dfrac{h_0}{\tau_{2w}}\right)\dfrac{\Delta N_w}{\Delta h} \end{pmatrix}}{\left(\dfrac{(1-h_0)}{\tau_{12}} + \dfrac{h_0}{\tau_{21}}\right)} \tag{14}$$

where $\frac{\Delta N_w}{\Delta h}$ is the variation between carrier density and ES occupation probability. It was obtained from the small-signal analysis of Eqs. (1). It is given by,

$$\frac{\Delta N_w}{\Delta h} = \frac{N_{w0}\left(\dfrac{1}{\tau_{w2}} + \dfrac{1}{\tau_{2w}}\right)}{\left(-i\,\delta + \dfrac{(1-h_0)}{\tau_{w2}} - \dfrac{h_0}{\tau_{2w}} + \dfrac{1}{\tau_{wr}}\right)} \tag{15}$$

So, Δf can be obtained from Eq. (13), f_0 can be taken from GS time series curve when it reaches steady-state. A similar procedure was also done for h_0 and N_{w0}. Then, the calculated f_0 and Δf were used into Eqs. (11) and (12) which were solved numerically.

IV. Conversion efficiency based on XGM

Assuming that $P_p(0)$ and $P_s(0)$ (in mW) are the input intensity of a pump and a probe pulses which are injected from the same facet of SOA while $P_p(L)$ and $P_s(L)$ are their values at the distance L from the input (at the end facet of the SOA). Let the frequency detuning between the two fields is larger than the inverse of stimulated carrier lifetime. Neglecting the four-wave mixing products induced by nonlinear interaction between the two fields. p_p and p_s are the small-signal harmonic modulations of P_p and P_s at frequency $\delta/2\pi$. At the input of the SOA, only the pump $P_p(0)$ was modulated, hence $p_p(0) \neq 0$ and $p_s(0) = 0$. Our aim was to calculate the modulation efficiency which is defined as [20]

$$\eta_{XGM} = \frac{p_s(L)}{P_s(L)}\frac{P_p(0)}{p_p(0)} \tag{16}$$

V. The quantum dot structure used in this study

The QD structure chosen in this study is (InAs) grown on $In_{0.53}Ga_{0.47}As$ WL, while the substrate is GaAs. This structure has been used by many research to study the different properties of QD [22,23]. It was assumed here that the disk has a radius of (14 nm) and a height of (2nm). The sub-bands energy of this QD structure are shown in the Fig. 1. The structure has two conduction sub-bands and four heavy hole (HH) valence sub-bands. The parameters were used in the calculations are in Table 1.

VI. Calculations, results and discussion

Figure 2 shows $\frac{\Delta N_w}{\Delta h}$ that was calculated from Eq. (15) which is reduced at wider detuning. Figure. 3 shows $\frac{\Delta f}{\Delta h}$ with detuning which increased at wider detuning. Figure 4 shows XGM conversion efficiency from QD SOA for different pulse widths for pump and probe pulses. For a short pump and probe pulses with FWHM equals (1ps) a high XGM efficiency was obtained. When the pump/probe width ratio increased,XGM is decreased, however, it increased with the reduction of pump/probe ratio. It is well known that QD SOAs can be driven to saturation by a short pulse. This increases the XGM efficiency. When the pulse width ratio between pump/probe increases, the saturation gain, and then efficiency increases. Accordingly, one can use the lower pump/probe ratio to obtain low (-3dB) bandwidth, i.e. low cross-talk. One can obtain high bandwidth with high pump/probe pulse width ratio. Note that increasing probe width is more efficient to increase bandwidth, as shown here, where an enough discrimination between curves is shown.

Fig. 5 shows XGM with probe power as a parameter. Increasing probe power reduces the efficiency. Each efficiency curve decline first, then, at ~10GHz it becomes flat. Additionally, XGM bandwidth decreases with increasing the probe power. It was observed experimentally that XGM in QD SOAs behavior attributes to the saturation features [18]. At low frequency, the modulation was due to the carrier density depletion in the WL carrier reservoir, where the overall gain spectrum is reduced. It was characterized by a slow recovery time. At high frequency,

SHB, which is characterized by fast recovery, was the dominant mechanism. Fig. 6 shows a comparison between calculated XGM efficiency from this model with experimental results from [12] where a good agreement was obtained.

VII. CONCLUSIONS

Theory of XGM in QD SOAs was discussed by combining the QD rate equation system with the pulse propagation into QD SOAs including the three region of QD structure GS, ES and the WL carrier reservoir. It was found that both WL reservoir and QD states contributedinto slow and fast recovery, respectively. It was found that the pump/probe pulse width ratio can be adjusted to control both efficiency and bandwidth.

Table 1. Parameters used in the calculation [6,9].

Parameter	Symbol	Value
Capture time from WL	$\tau_{w\,2}$	3 ps
Escape time from ES to WL	τ_{2w}	1 ns
capture time from ES to GS	τ_{21}	0.16 ps
Escape time from GS to ES	τ_{12}	1.2 ps
Recombination time	τ_{1r}	0.4 ns
Group refractive index	n_g	3.6
surface carrier density	NQ	$10^{15}\ m^{-2}$
Thickness of dot layer	L_w	10 nm
Amplifier width	w	$2\mu m$
Amplifier length	L	3 mm
pump wavelength	λ_0	1.3 μm
optical Confinement factor	Γ	0.027
Temperature	T	300 k

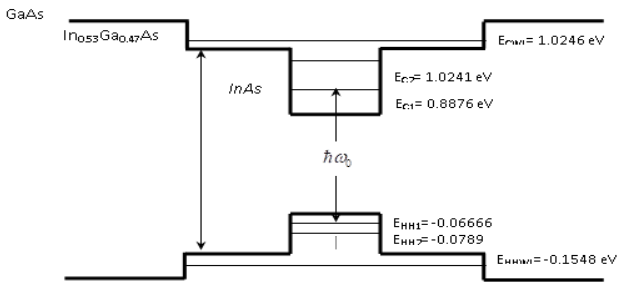

Fig. 1:The band structure of ($InAs$ / $In_{0.53}Ga_{0.47}As$ / $GaAs$)QD.

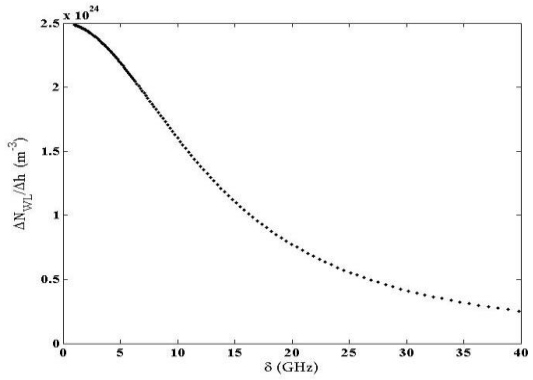

Fig. 2 The variation of (WL carrier density/ES occupation) versus detuning.

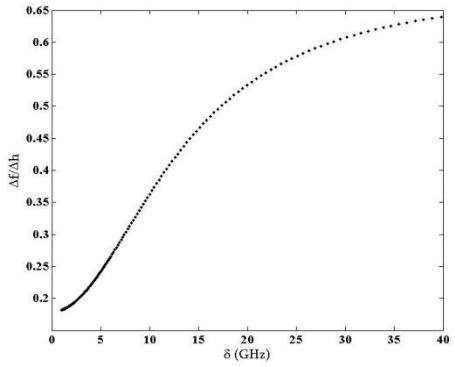

Fig. 3. The variation of (GS occupation/ES occupation) versus detuning.

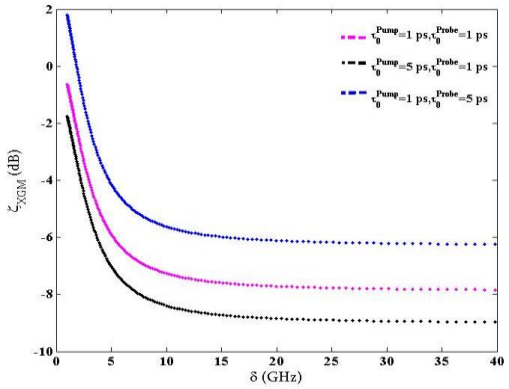

Fig. 4. XGM conversion efficiency at different pulse width of pump and probe.

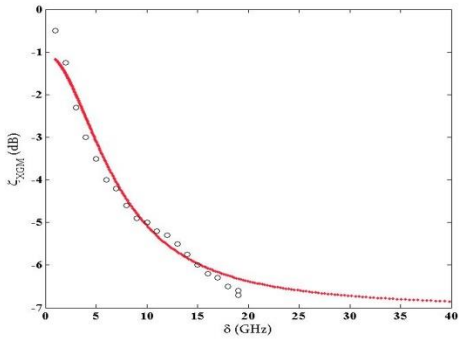

Fig. 5. XGM conversion efficiency at 0.2mW pump power and different powers of probe pulse.

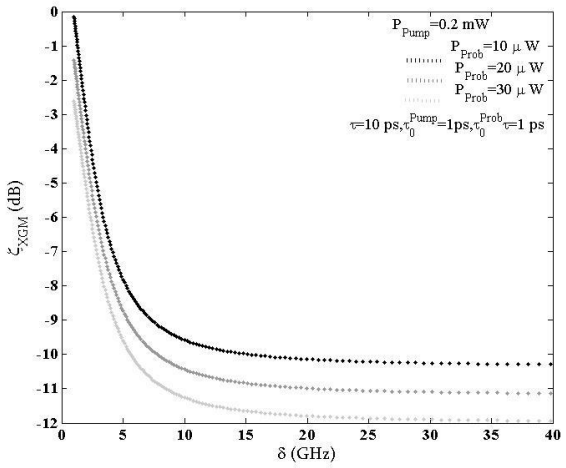

Fig. 6. Comparison between theoretical and experimental XGM efficiency. Open circles are for experimental data which is taken from [12].

CONFLICT OF INTEREST

Authors declare that they have no conflict of interest.

REFERENCES

[1] D. Pastor, A. Martinez, J. Capmany, Salvador. Sales, B. Ortega, and P. Munoz, "Experimental characterization of XGM-SOA-based wavelength converted SCM systems", *IEEE Photonics Technology Letters* 15, 2003, 114-116.

[2] W. Zhaoxi, H. Yuanqing, W. Zihua,Y. Ruifang, "All-optical wavelength conversion based on cascaded effect of cross gain modulation and cross-phase modulation in SOAs", *SPIE* 6625, 2008, 66251V1-8.

[3] T. Durhuus, B. Mikkelsen, C. Joergensen, and K. E. Stubkjaer, "All optical wavelength conversion by semiconductor optical amplifiers", *J. Lightwave Technol.,* 14, 1996, 942–954.

[4] Y. Ben Ezra, B. I. Lembrikov, and M. Haridim, "Specific features of XGM in QD-SOA", *IEEE J. Quantum Electronics* 43, 2007, 730-737.

[5] G. Contestabile, R. Proietti, N. Calabretta, and E. Ciaramella, "Cross-gain compression in semiconductor optical amplifiers", J. Lightwave Technology 25, 2007, 915-921.

[6] G. P. Agrawal, Fiber Optic Communication Systems, 3rd ed. New York: Wiley, 2002.

[7] H. Lee, H. Yoon, Y. Kim, and J. Jeong, "Theoretical study of frequency chirping and extinction ratio of wavelength-converted optical signals by XGM and XPM using SOAs*", IEEE J. Quantum Electronics* 35, 1999, 1213–1219.

[8] S. Xu, J. B. Khurgin, I. Vurgaftman, and J. R. Meyer, "Reducing crosstalk and signal distortion in wavelength-division multiplexing by increasing carrier lifetimes in semiconductor optical amplifiers," J. Lightwave Technology 21, 2003, 1474–1485.

[9] D. Nielsen, S. L. Chuang, N. J. Kim, D. Lee, S. H. Pyun, W. G. Jeong,
C. Y. Chen, and T. S. Lay , 'High-speed wavelength conversion in quantum dot and quantum well semiconductor optical amplifiers', Applied Physics Letters 92, 2008.

[10] M. Sugawara, H. Ebe, N. Hatori, M. Ishida, Y. Arakawa, T. Akiyama, K. Otsubo and Y. Nakata, "Theory of optical signal amplification and processing by quantum-dot semiconductor optical amplifiers" , Phys. Rev. B 69, 2004.

[11] P. S. Cho and J. B. Khurgin, " Suppression of Cross-Gain Modulation in SOA Using RZ-DPSK Modulation Format", IEEE Photonics Technology Letters 15, 2003, 162-164.

[12] J. Kim and S. L. Chuang, "Small-signal cross-gain modulation of quantum-dot semiconductor optical amplifiers", *IEEE Photonics Technology Letters* 18, 2006, 2538 -2540.

[13] F. Keshavarz and V. Ahmadi, "High-Speed Pattern Effect Free Cross-Gain Modulation in QD-VCSOA", *J. Lightwave Technology* 30, 2012, 3043-3049.

[14] J. Kim, C. Meuer, D. Bimberg, and G. Eisenstein, "Numerical simulation of temporal and spectral variation of gain and phase recovery in quantum-dot semiconductor optical amplifiers", *IEEE J. Quantum Electronics* 46, 2010, 405-413.

[15] A. Bilenca, R. Alizon, V. Mikhelashhvili, D. Dahan, G. Eisenstein, R. Schwertberger, D. Gold, J. P. Reithmaier, and A. Forchel, "Broad-band wavelength conversion based on cross-gain modulation and four-wave mixing in InAs–InP quantum-dash semiconductor optical amplifiers operating at 1550 nm", *IEEE Photonics Technology Letters* 15, 2003, 563-565.

[16] M. Matsuura, O. Raz, F. Gomez-Agis, N. Calabretta, and H. J. S. Dorren, "Ultrahigh-speed and widely tunable wavelength conversion based on cross-gain modulation in a quantum-dot semiconductor optical amplifier," Opt. Exp. 19, 2011, B551–B559.

[17] G. Contestabile, A. Maruta, S. Sekiguchi, K. Morito, M. Sugawara, and K. Kitayama, " Cross-gain modulation in quantum-dot SOA at 1550 nm", *IEEE J. Quantum Electronic*s 46, 2010, 1696-1703.

[18] C. Meuer, J. Kim, M. Laemmlin, S. Liebich, G. Eisenstein, R. Bonk, T. Vallaitis, J. Leuthold, A. Kovsh, I. Krestnikov, and D. Bimberg, "High-speed small-signal cross-gain modulation in quantum-dot semiconductor optical amplifiers at 1.3 μm", *IEEE J.*

Selected Topics in Quantum Electronics 15, 2009, 749-756.

[19] O. Qasaimeh, "Characteristics of cross-gain wavelength conversion in quantum dot semiconductor optical amplifiers," *IEEE Photon. Technol. Lett*., 16, 2004, 542–544.

[20] A. Mecozzi, "Small-signal theory of wavelength converters based on cross-gain modulation in semiconductor optical amplifiers", *IEEE Photonics Technol. Lett.* 8, 1996, 1471–1473.

[21] M. Sugawara, T. Akiyama, N. Hatori, Y. Nakata, K. Otsubo, and H. Ebe, "Quantum-dot semiconductor optical amplifiers", *Proceedings of SPIE*, 4905, 2002, 259-275.

[22] S. L. Chuang, "physics of optoelectronics", John Wiley & Sons, USA, PP. (708-711), 1995.

[23] S. Adachi , "Properties of Group-IV, III–V and II–VI semiconductors" , Japan, 2005.